Effect of hydrogen redistribution during aging on the structure and phase state of nanocrystalline and coarse-grained TiNi alloys

Anatoly Baturin [a, b, *], Aleksander Lotkov [a], Victor Grishkov [a], Ivan Rodionov [a], Victor Kudiiarov [b]

[a] Institute of Strength Physics and Materials Science SB RAS, 2/4, pr. Akademicheskii, 634055, Tomsk, Russia
[b] Tomsk Polytechnic University, 30, Lenin Avenue, 634055, Tomsk, Russia

ARTICLE INFO

ABSTRACT

The report presents research data showing how the phase state and transition temperatures in hydrogenated nanocrystalline and coarse-grained TiNi alloys are influenced by hydrogen redistribution on their aging at room temperature. The research methods include four-point measurements of resistivity as a function of temperature and differential scanning calorimetry at 173—373 K. The results demonstrate that hydrogen diffusion in the material bulk provides gradual suppression of $B2 \rightarrow B19'$ and $R \rightarrow B19'$ transformations and that the temperature of $B2 \rightarrow R$ transformation is hardy sensitive to hydrogen. Also presented is an analysis of the mechanism by which hydrogen acts on the temperatures and sequence of martensite transformations.

© 2018 Elsevier B.V. All rights reserved.

1. Introduction

Freshly hydrogenated TiNi alloys show degradation of their superelasticity and shape memory effect, higher critical stress for phase transitions and hydrogen embrittlement [1—3].

Hydrogenation is generally electrolytic and consists in cathodic hydrogen charging. Immediately after the process, most of the hydrogen in TiNi is concentrated in its near-surface layer, which is substantially hardened, and this causes hydrogen embrittlement [4]. On further aging at room temperature, the hydrogen is redistributed by diffusion over the material, and this can greatly change its superelastic and mechanical properties [5].

Because superelasticity, shape memory effect, and their temperature range in TiNi alloys are governed by thermoelastic martensite transformations, we are to know how hydrogen influences the temperatures and sequence of such transformations in TiNi aged at room temperature. Research data on a hydrogenated ternary TiNi alloy ($Ti_{50}Ni_{30}Cu_{20}$) show that its long-term aging

slightly lowers the temperature of direct martensite transformation and decreases the transformation enthalpy [5]. The effect of long-term aging on martensite transformations in hydrogenated binary TiNi alloys has not been studied so far.

Here we analyze the temperatures and sequence of martensite transformations in a hydrogenated $Ti_{49.1}Ni_{50.9}$ alloy with nanocrystalline and coarse-grained structure depending on the time of aging at room temperature.

2. Experimental

The test specimens were $Ti_{49.1}Ni_{50.9}$ wires (at%) of diameter 1.1 mm (MATEK-SMA, Russia) hydrogenated in a 0.9% NaCl solution at a current density of 20 A/m^2 for 3 h. The microstructure of the specimens was analyzed by scanning (LEO EVO 50) and transmission (JEM-2100) electron microscopy.

The hydrogen concentration was measured with a gas analyzer (LECO RHEN 602). Its value in the specimens immediately after hydrogenation was 400—430 wt ppm in the nanocrystalline samples and 200—250 wt ppm in the coarse-grained samples. The effect of aging on the sequence and temperatures of martensite transformations was studied by two methods: four-point

* Corresponding author. Institute of Strength Physics and Materials Science SB RAS, 2/4, pr. Akademicheskii, 634055, Tomsk, Russia.
    E-mail address: abat@ispms.tsc.ru (A. Baturin).

measurements of resistivity as a function of temperature $\rho(T)$ in the range 83–333 K and differential scanning calorimetry (Mettler Toledo 822) in the range 173–373 K. The heating and cooling rates were 10 °C/min.

3. Research results

3.1. Initial microstructure

The wires after drawing had nanocrystalline structure with an average grain size of 86 nm dominated by near-equiaxed grains with high-angle misorientations (Fig. 1a, b, c). To obtain coarse-grained specimens, the wires were annealed at 973 K for 30 min and quenched in water such that the average size of equiaxed grains was 10 μm (Fig. 1d, e).

3.2. Martensite transformations in nanocrystalline and coarse-grained TiNi

Fig. 2 shows the temperature dependence of resistivity and calorimetric curves for the initial nanocrystalline material. Such curves of resistivity and heat flow are characteristic for B2↔R↔B19′ transformations in binary TiNi alloys rich in nickel with respect to their equiatomic composition. The transformation temperatures are marked by arrows in Fig. 2a: M_s and M_f are the start and finish temperatures of direct R→B19′ transformation; A_s

and A_f are the start and finish temperatures of reverse martensite transformation; and T_R is the temperature of B2→R transformation.

The transformation temperatures for the nanocrystalline material are $T_R = 264$ K, $M_s = 212$ K, $M_f = 182$ K, $A_s = 236$ K, and $A_f = 252$ K. According to differential scanning calorimetry, $T_R = 274.2$ K, $M_s = 207.3$ K, $M_f = 181.2$ K, $A_s = 252.5$ K, and $A_f = 262.4$ K. The two methods demonstrate the same sequence of martensite transformations, and their temperatures coincide accurate to ±5 deg. The transformation enthalpy ΔH is 4.81 J for B2→R, 16.39 J for R→B19′, and 19.09 J for B19′→B2. The high value of ΔH for reverse B19′→B2 transformation is likely because R→B2 transformation may occur in about the same temperature range.

Fig. 3 shows the temperature dependence of resistivity $\rho(T)$ for the coarse-grained material. Such a form is characteristic for B2↔B19′ transformations in binary TiNi alloys rich in nickel with respect to their equiatomic composition. The change in $\rho(T)$ before M_s features a negative temperature coefficient of resistivity and owes to premartensitic phenomena [6]. The transformation temperatures for the coarse-grained material are $M_s = 241$ K, $M_f = 221$ K, $A_s = 252$ K, and $A_f = 263$ K.

3.3. Martensite transformations in hydrogenated and aged TiNi

After hydrogenation and subsequent aging at room temperature for half a year, the dependence $\rho(T)$ reveals radical changes: no
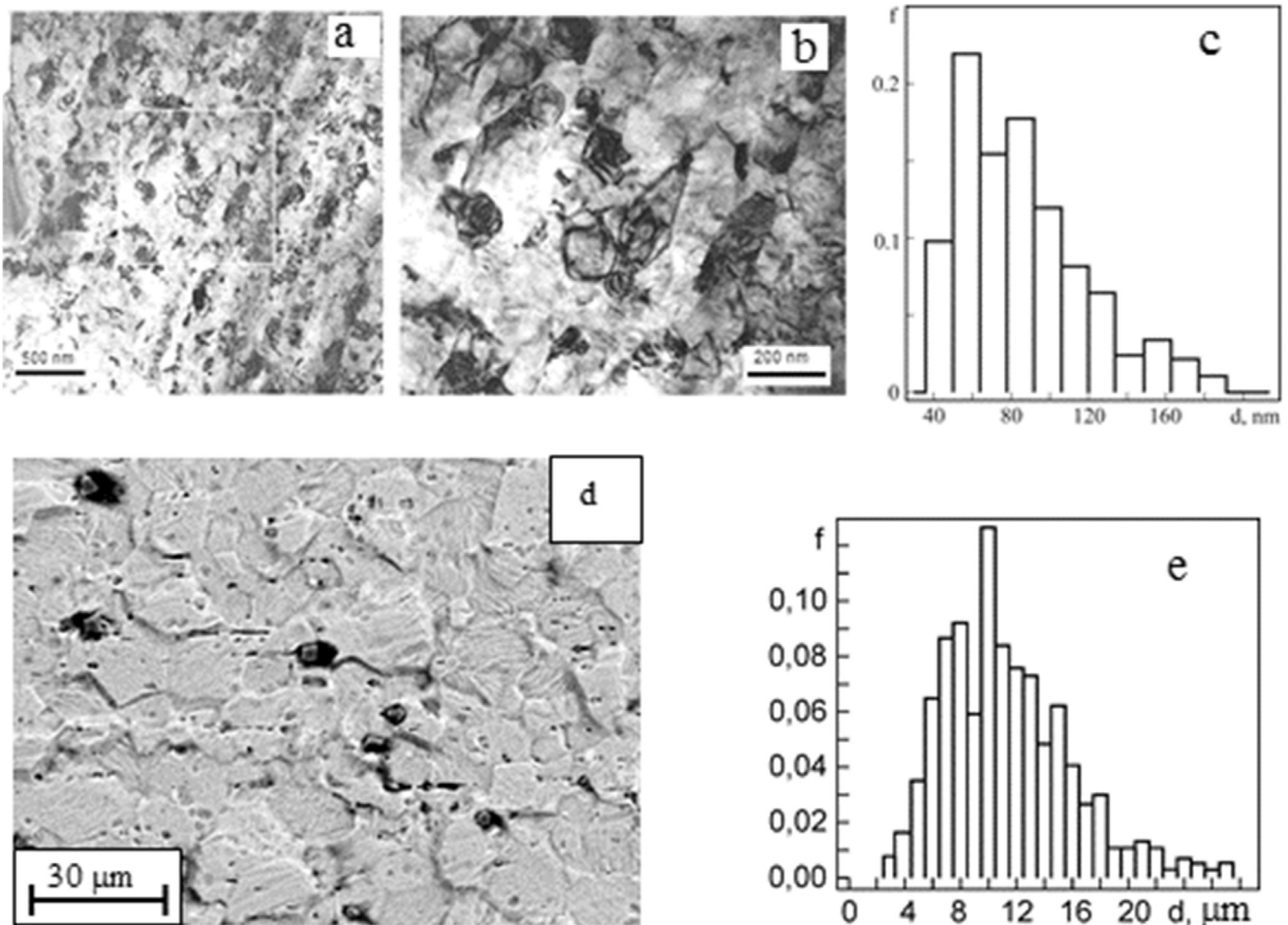

Fig. 1. Microstructure and grain size distribution in nanocrystalline (a, b, c) and coarse-grained Ti$_{49.1}$Ni$_{50.9}$ (d, e).